Design and Analysis of Diagnostic Machines

Utilizing Compliant Mechanisms
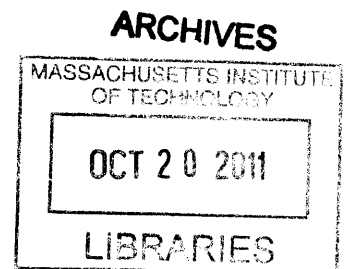
by

Edward Sung

Submitted to the Department of Mechanical Engineering
in Partial Fulfillment of the Requirements for the
Degree of

Bachelor of Science

at the

Massachusetts Institute of Technology

June 2011

Signature of Author ....
Department of Mechanical Engineering
December 8, 2010

Certified by ....
Martin L. Culpepper
Associate Professor
Thesis Supervisor

Accepted by ....
John H. Lienhard V
Samuel C. Collins Professor of Mechanical Engineering
Undergraduate Officer

Design and Analysis of Diagnostic Machines

Utilizing Compliant Mechanisms

by

Edward Sung

ABSTRACT

In this paper, the design and testing of an ankle rehabilitation device is presented. The purpose of the research done is to provide physicians with a diagnostics tool that can quantitatively measure the severity of an injury by measuring the ankle joint's functional output. Torque and power output have been shown to be correlated with functional performance of the ankle joint. The device can measure torque and power output over the full range of motion of the ankle joint complex. Such a device has the potential to enable more accurate diagnoses and improve the efficacy of treatment and rehabilitation.

The device allows rotation about the three orthogonal axes in the Cartesian plane. The rotations are linked in series to simulate ankle subjoint coupling. Cartwheel flexures with strain gages are aligned with the rotational axes and used as torque sensors. Strain gages are placed in a Wheatstone bridge circuit to mitigate environmental factors.

Trials measured torque of the right ankle joint of test subjects from a standing position. Results show that the coupling of the two modes of ankle joint rotation (plantarflexion/dorsiflexion and inversion/eversion) are dependent on a subject's own development.

Thesis Supervisor: Martin L. Culpepper

Title: Associate Professor

ACKNOWLEDGEMENTS

First and foremost I would like to thank my thesis advisor Professor Martin L. Culpepper of the Precision Compliant Systems Laboratory (PCSL) at MIT for providing all of the advice and support that I needed to complete a successful thesis.

I would like to thank Alex Slocum Jr., a graduate researcher formerly of the PCSL, for his substantial help with the ankle rehabilitator project. He worked closely with me and my partner, Raymond Ma '10, and we could not have done this without him.

A special thank you goes out to Raymond Ma for his work on the initial prototype and the electronics. Finally, I would like to extend my gratitude to Dr. Jonathan Bean for making this project possible through his medical insight and monetary support.

CONTENTS

FIGURES

TABLES

1

INTRODUCTION

1.1 Purpose

The purpose of this work is to provide clinicians with an accurate and reliable tool for diagnosing ankle injuries. Injuries to the Ankle Joint Complex (AJC) are one of the most common types of orthopedic injuries, generally experienced most often by athletes or the elderly. Torque and power output of the ankle joint have been shown to be correlated with functional capability [1]. A device that can measure both power and torque output of the ankle joint has the potential to enable a more accurate diagnosis and also improve the efficacy of a given rehabilitation regimen.

The device that has been developed is shown in figure 1.1. Torque is measured using cartwheel flexures, which have their flexure blades positioned radially so as to only allow angular displacement. The rotational axes of the flexures are aligned with those of the AJC, thus simulating AJC motion. Strain gages on the flexure blades give a voltage reading proportional to the torque applied. After calibration, the relationship between applied torque and angular displacement will also be known. Angular displacement can be differentiated with respect to time in order to calculate angular velocity, and therefore power (torque x angular velocity).
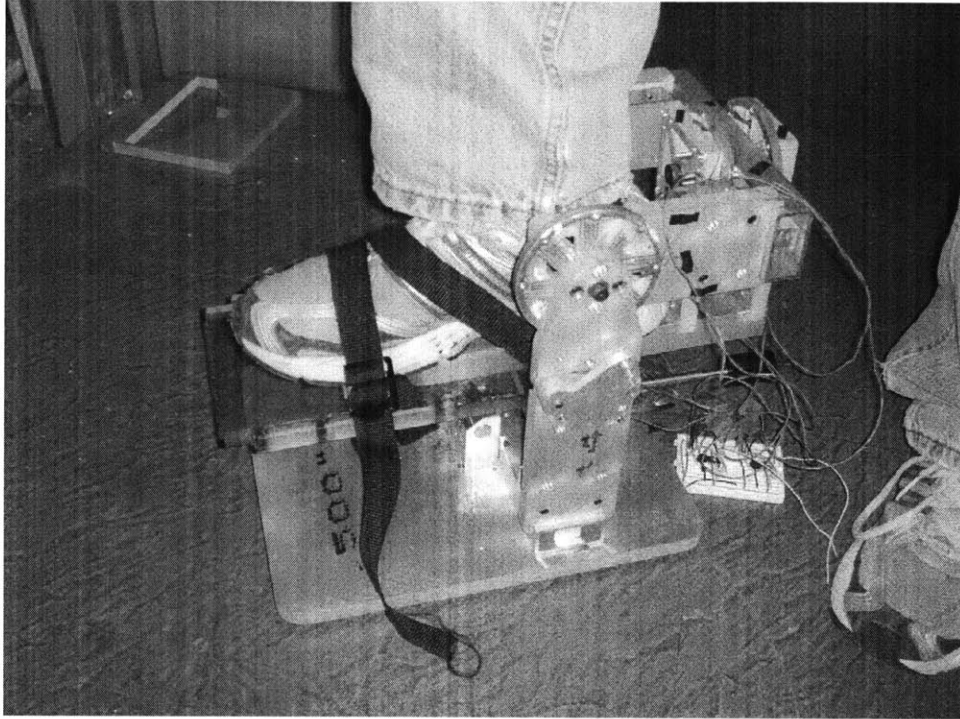
Figure 1.1: The ankle rehabilitation device

1.2 Background

AJC performance is also often used as an indicator of neuromuscular impairment, due to the importance the joint plays on balance [2]. However, current methods for the diagnosis and treatment of such injuries are varied in their efficacy. Current diagnostic procedures rely on the subjective assessment of a clinician in order to determine both the initial severity of an injury as well as the extent to which an injury has healed [3].

The subjective nature of this processes results from the clinician's reliance on patient response to questions relating to pain and ease of motion. While the responses may be used as a general guideline to determine the amount of rest or rehabilitation the patient should undergo, responses are also usually affected by factors such as the patient's own pain tolerance, or their

own ability to accurately describe their symptoms. Current clinical practice has few quantitative

physical assessment tools that are both reliable and repeatable [4].

1.2.1 Existing Devices

Noteworthy devices with quantitative diagnostics capabilities are the gait pressure device,

the Rutgers Ankle Interface, and the handheld dynamometer [5-8]. Figure 1.2 shows how each

device is used. Tables 1.1-1.3 shows a comparison of the 3 devices with their pros and cons

listed below each device.
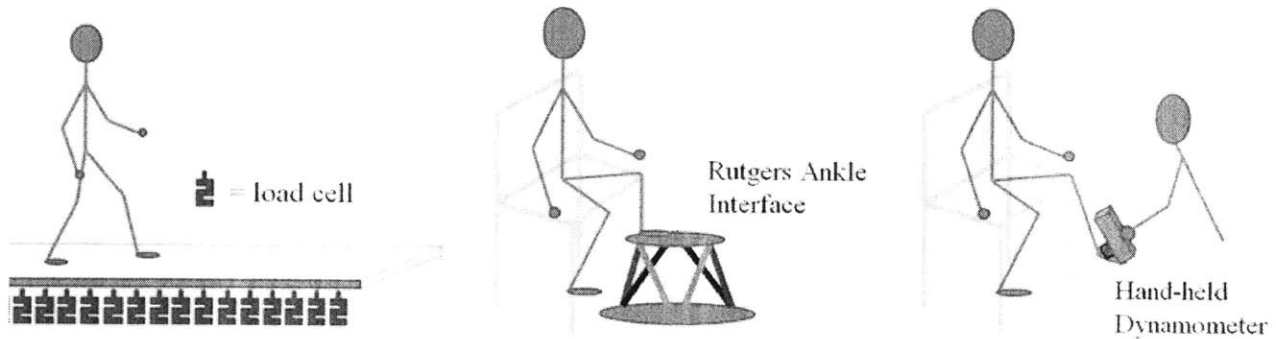
Figure 1.2: Gait Pressure Device (left), Rutgers Ankle Interface (middle), Hand-held Dynamometer (right)

Table 1.1: Gait Pressure Device characteristics

Vendor	Zebris, Bertec, etc.
Usage	Measure foot-ground reaction forces and center of foot pressure during gait.
Method	Measures gait pressure using multiple load cells placed in a treadmill[5].
Limitations	Does not analyze ankle kinematics [5].
	Cannot measure position or angular velocity of ankle rotation [5].
	High cost.

10

Table 1.2: Rutgers Ankle Interface characteristics

Vendor	N/A
Usage	Personal device for in-home use. Move ankle joint through a range of motion and measure load capacity.
Method	A pseudo-passive Stewart Platform uses double-acting pneumatic cylinders to move the foot through a ROM and measure load bearing capability [6].
Limitations	Low force output and input. Cannot exert larger forces on foot [6] and cannot support weight of patient [7]. Low reliability due to vibrations, large temperature fluctuations, and overheating of compressor [6]. High cost (projected).

Table 1.3: Hand-held Dynamometer characteristics

Vendor	Hoggan, Jamar, etc.
Usage	Measure torque of joint to which device is held.
Method	Load cell, electric motor, etc.
Limitations	Variability between repeated measures [8]. Variability between various dynamometers [8]. Hoggan, Jamar, etc.

2

METHODS

2.1 Kinematics of the Ankle Joint (AJC)

Because we wish to directly measure the torque output of the AJC, a good understanding of anatomy and the kinematics of the joint is required. The AJC is actually comprised of two subjoints, the true ankle joint and the subtalar joint. Each of these subjoints allows rotation about a single axis. The true ankle joint is responsible for motions such as plantarflexion and dorsiflexion, and the subtalar joint is responsible for inversion and eversion joint motions. As is shown in Figure 2.1, the true ankle joint is located above the subtalar joint; the reader can locate their own subtalar joint at the protruding end of the fibula, on the medial (inner) side of the AJC. It is important to note that the two subjoints are connected in series, and therefore their rotations are uncoupled. Specifically, plantarflexion of the joint and then joint inversion results in a different set of motions from inverting prior to plantarflexing. [9]
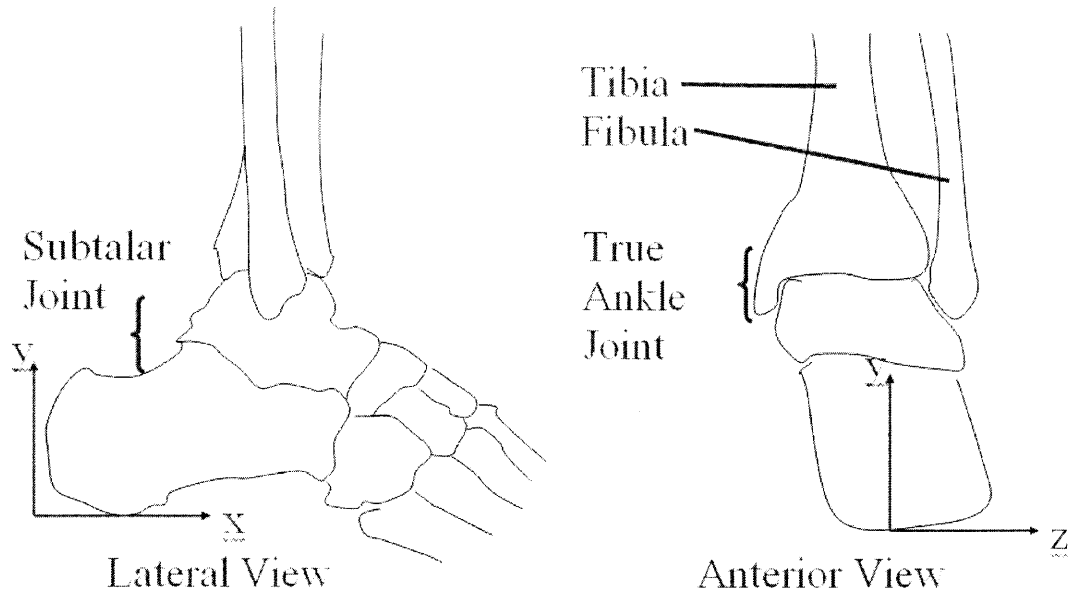
Figure 2.1: Ankle Joint Complex

The axis convention shown in Figure 2.1 will be used. The x and z axes in the figure will form the ground plane; the x-axis is aligned with the longitudinal direction of the foot, and the y-axis is aligned vertically, about which there are two sources of rotation. The primary source is tibial/fibula movement, which is not actually a rotation in the AJC. When the lower leg is held still, the AJC provides rotation about the y-axis via a combination of motions of the two subjoints. When the foot is rotated inward, while constraining the lower leg, the motion that is seen is actually a combination of plantarflexion and inversion. It is for this reason that during such motion, the flat of the foot cannot be held parallel to the ground and will be observed to tilt up at an angle.

While the range of motion (ROM) of the AJC can be characterized using the axes of the subtalar and true ankle joints, it is still necessary to be able to measure the load capacity in the rotational direction about the y-axis for certain injuries. A low load capacity or pain upon

13

movement can indicate damage of skeletal tissue in the vicinity of the AJC. As such, the device will have torque sensors measuring torque in all three rotational directions, θ_x, θ_y, and θ_z.

2.2   Torque Sensor

It was postulated to use cartwheel flexures as torque sensors. A basic cartwheel flexure, along with its basic deformation geometry, is shown in figure 2.2.

strain gages
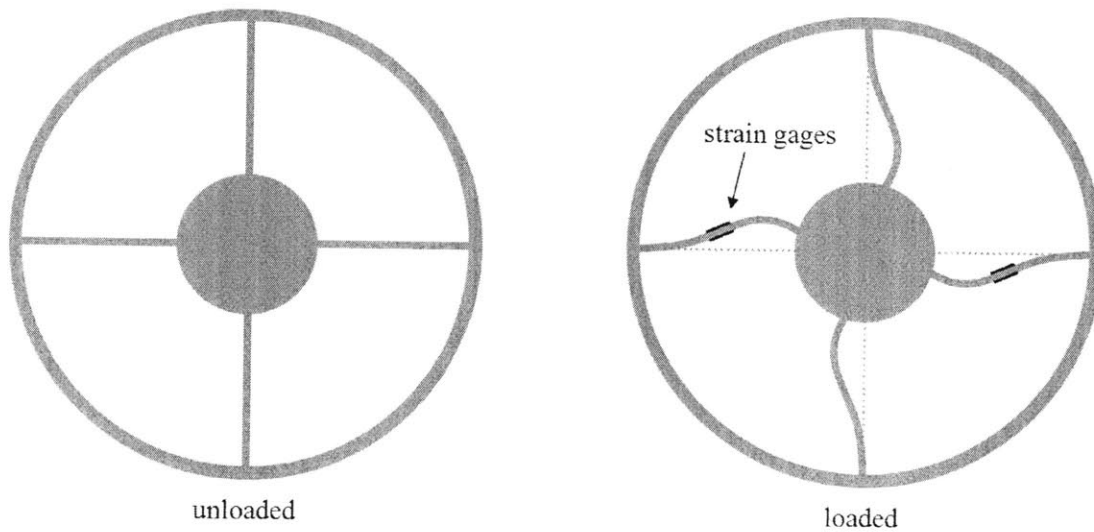
unloaded   loaded

Figure 2.2: Cartwheel flexure in unloaded configuration (left), and approximate deformation mode (right)

Strain gages are bonded to the flexure blades. In order to mitigate environmental factors such as temperature fluctuations, the strain gauges are placed in a Wheatstone bridge circuit. The outer ring of the cartwheel flexure grounded while the inner ring is rigidly attached to the rotation of the patient's foot, creating measurable deflection in the blades of the cartwheel flexure.

The torque applied to the sensor is linearly related to strain, which makes the flexure modules simple to calibrate using the process detailed by Ma [10]. The calibration is done by bolting a lever arm to the inner ring and hanging increasing loads from the end of the lever. This yields the constant K in the equation $\theta = K * T_{applied}$. During calibration, the relationship

14

between torque and angular rotation is also recorded. Thus for a given strain reading, both the applied torque and the resulting angular rotation can be calculated, which can be differentiated to find angular velocity and power. Simple cantilevered-beam deflection models can be used to calculate force.

2.3 Device Protocols

The cartwheel flexures are set up as shown in Figure 2.3. The first round of preliminary tests have been completed. The subject stands on the platform with one foot strapped in and the other resting on another platform of equal height. Then the subject applies as much force as possible for a few seconds each in first plantarflexion, then dorsiflexion, then inversion, and last eversion. This gives us the maximum torques in each mode of rotation. For power readings, the subject applies a high impulse, forcing the foot plate to rotate as fast as possible.

plantar dorsiflexion
flexures

inver eversion
flexures

foot

heel
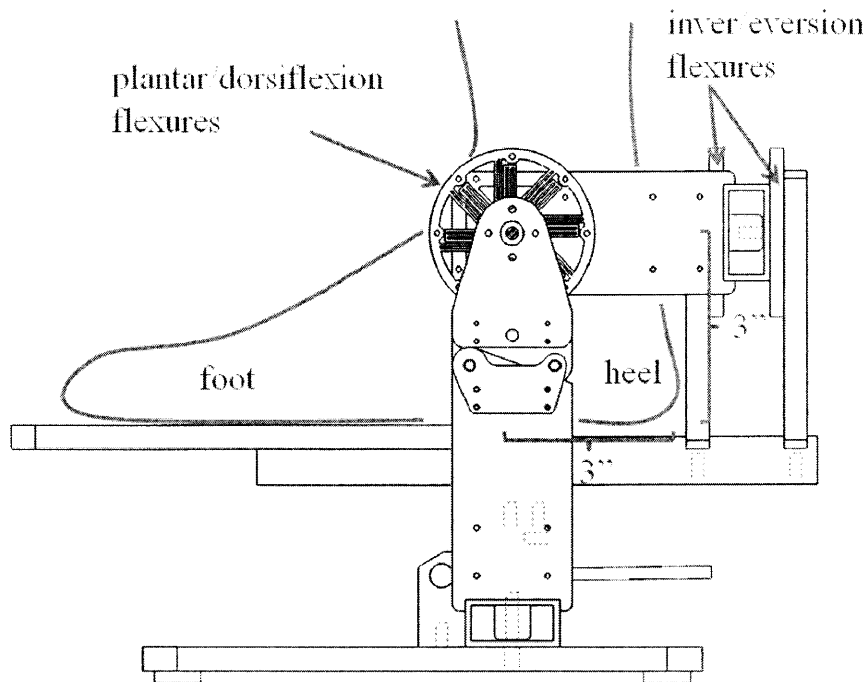
Figure 2.3: Prototype with flexures

Other protocols that test the functional strength of the ankle joint are being investigated and will be implemented during a clinical, for which preparations are currently being made. Among the protocols to be evaluated are the Starr-Excursion Balance test (SEBT) and the Unipedal Stance test (UST). Range of motion cannot be measured easily with the current prototype, so this study will focus on validation. Improvements will be made so that in future prototypes, the range of motion will be measured through either one of two methods: (1) extremely large motion flexures (>0.5 rad); (2) a semi-automated process that depends on the torque applied. For method (2), as long as the torque applied is above a certain number, a motor will rotate the foot plate slowly; when the torque applied falls below that number, the motor will stop, and the limit of the AJC's ROM will be measurable with just the flexure's ROM.

3

DESIGN AND BUILD

3.1 Functional Requirements

The first step in the design process was to establish the functional requirements for the

device, which are listed in table 3.1. The functional requirements were mostly dependent on what

the customer wanted the device to do.

Table 3.1: Functional Requirements for the Ankle Rehabilitation Device

Functional Requirement	Reason
1. Simulate AJC motions (zero translational DOFs and all three angular DOFs) from a given foot position; rotate ~0.09 rad in each DOF when the foot position is set	Large displacements are required to calculate power readings. Additionally, an interface that doesn't give under load will stress the ankle joint and cause more pain than is necessary
2. Accommodate up to size 15 (US) feet	The 99th percentile shoe length is 330 mm [11]
3. Support a load of up to 91 kg	This is the maximum weight we expect a test subject to exert on the device
4. Be adjustable to different foot positions within the range of 0.8 rad / 0.2 rad for plantar/dorsiflexion and 0.8 rad / 0.2 rad for inver/eversion	The device must be able to measure ankle output throughout the ROM of the ankle
5. Accommodate different foot anatomy with variations of up to 15 mm in the vertical distance between the true ankle joint and the subtalar joint, and 25 mm in the vertical and horizontal distances between the subtalar joint and the bottom of the shoe	Different patients have different developments in their feet and AJC. Additionally, shoe sizes vary greatly

6. Have stiff flexures with maximum angular displacement of 0.00015 rad for pseudo-static measurement in certain tests such as the unipedal stance test	The platform must feel like it is as stable as the ground so that the patient does not falter or feel unstable while balancing on one leg.
7. Be able to switch out flexures for different tests within 60 seconds	Functional requirements 2 and 7 require different flexures.

It should be noted that requirements 1-4 were functional requirements for the β-prototype. Functional requirements 5-7 were added to accommodate feedback from users and to address shortcomings of the machine identified during experiments.

3.2 Design Concepts

Using the initial functional requirements (1-4), design concepts were generated. These are discussed in the following sections.

3.2.1 3-Axis Rotation in Series

The β-prototype currently being used is based off of this concept. This concept mimics ankle motion by having its rotations in series in the same order as those of the AJC. That is, ground, the first stage, is connected to a second stage that rotates about the y-axis. Then the second stage connects to a third stage that rotates about the z-axis. Finally, the third stage connects to a fourth and last stage that rotates about the x-axis. A rendered model of the initial concept is shown in Figure 3.1.

18
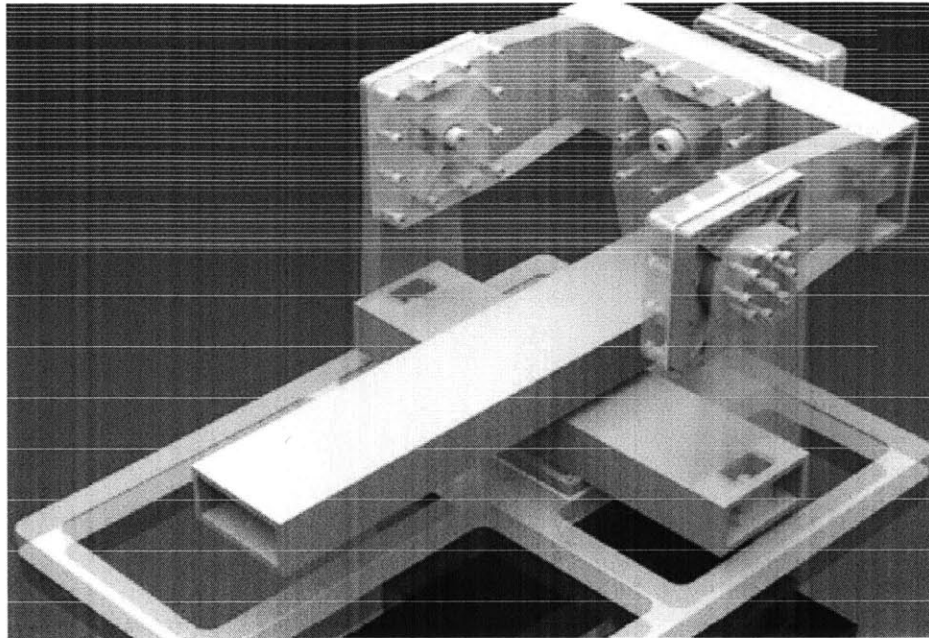
Figure 3.1: 3-axis rotation in series concept

3.2.2 Nested 4-Bar Linkages

A 4-bar linkage has the property that, when the bottom linkage is fixed, the top linkage rotates about a point in space which is the intersection of the extended side linkages. By adjusting the angles or the lengths of the side linkages, it is possible to adjust the height of the point in space. While the point of space does shift during motion, for a point 102 mm above the top linkage and for 0.09 rad of rotation, it does not shift more than 2.5 mm, which is not significant. The ROM of the AJC can be simulated by placing one 4-bar linkage on top of another 4-bar linkage, but rotated 1.57 rad so as the rotations are perpendicular to each other. There is also the option of nesting the 4-bar linkage such as is shown in figure 3.2. This allows the rotations to be decoupled and be independent of each other.
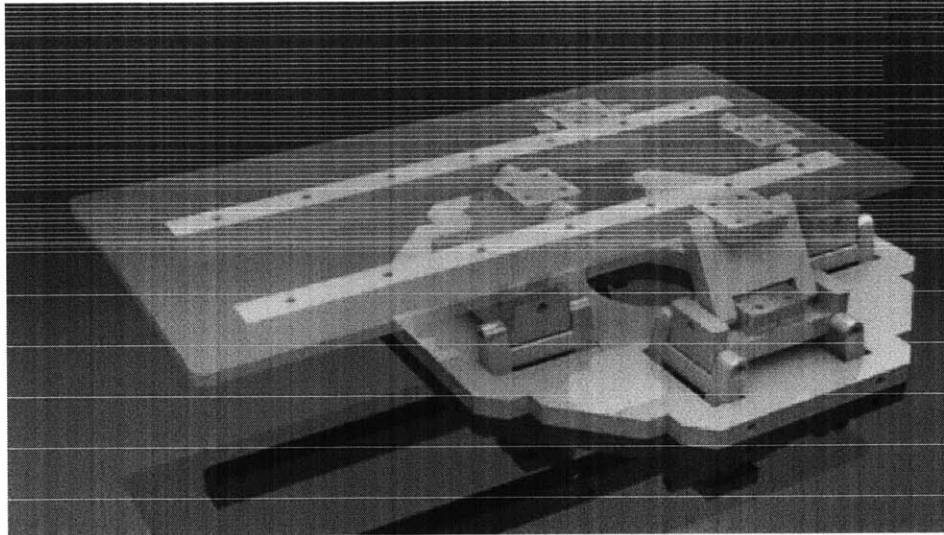
Figure 3.2: Nested 4-bar linkages concept

Ergonomically, this design has the advantage that the flexures do not have to be in line with the rotational axes. This allows the device to be much more compact and for there to be no components that might come into contact with the patient. With the 3-axis design, the components have to be sufficiently large to ensure that no contact occurs. That also means that any foot position adjustment mechanisms have to be integrated into the flexure modules instead of being able to tilt the entire torque sensing platform, forcing the design to be complex. The 4-bar linkage design has no such complications and can be placed on a separate independent platform that changes position.

3.2.3 Concept Assessment: Weighted Cost-Comparison Chart

Although the 4-bar linkage design seems to hold promise, after careful evaluation of each concept with respect to the functional requirements, it was determined, using the weighted cost-comparison chart shown in Table 3.2, that the 3-axis design fit our requirements better. However,

this evaluation was based only on functional requirements 1-4. The assessment result might differ with the additions of requirements 5-7.

Table 3.2: Weighted cost-comparison chart of concepts

	cost	manufacturability	position adjustment	data interpretation	flexure ROM	AJC simulation	Score
weight	2	1	2	2	3	3	N/A
3-axis	2	2	1	3	3	3	32
4-bar	3	2	3	1	1	3	27

At the point of time of this assessment, we were unable to design a flexure for the 4-bar design that would allow a rotation of 0.09 rad. Even if such a flexure were viable, we would run into an issue with data interpretation. Because the flexure blades for the 4-bar design are placed radially far out from the center of rotation, the blades must deflect much more than the blades in a cartwheel flexure in order to achieve the same rotation. For large deflections, it is likely that the relationship between torque, strain, and angular deflection is nonlinear. This would result in a very extensive and complicated calibration process.

3.3 α-Prototype

In the spring term of 2009, the α-prototype shown in Figure 3.3 was constructed by a student colleague. All of the components were cut on an OMAX waterjet from one 7.9 mm sheet of 6061-T6. While the material cost was very low, the structure did not have enough rigidity to constrain deflections to just the flexures. The structure also could not support more than 5 kg and the deflections resulted in significant errors in the data. Additionally, large loads resulted in significant translational forces on the flexure blades. In order to minimize error, the loads on the flexure blades must be pure torque. In the β-prototype, this issue is addressed by the usage of

shoulder bolts and bushings to eliminate the translational degree of freedom in the mechanism and support the patient's weight.
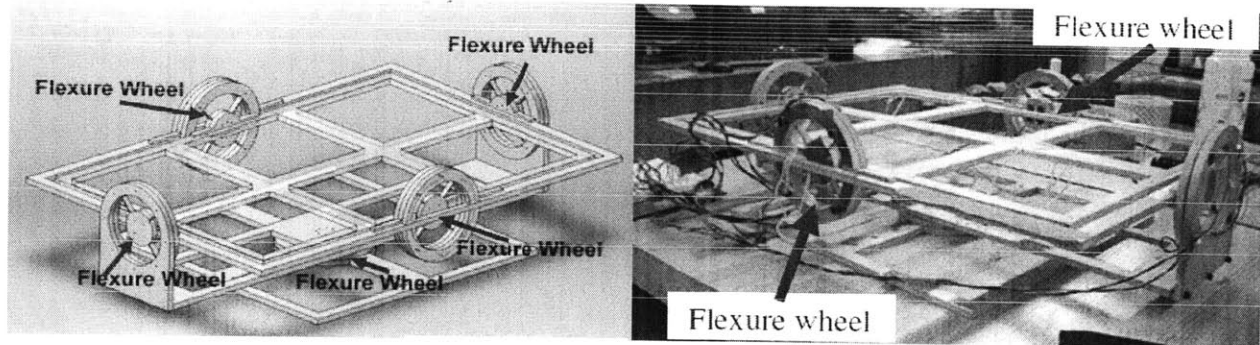
Figure 3.3: α-prototype [12]

The same cartwheel flexure design was implemented, with minimal changes for the β-prototype. The dimensions and locations of the flexure blades were kept constant, while the outer ring was changed to a square shape to enable better nesting for waterjetting and for placement within the device. This new cartwheel flexure is shown in Figure 3.4.
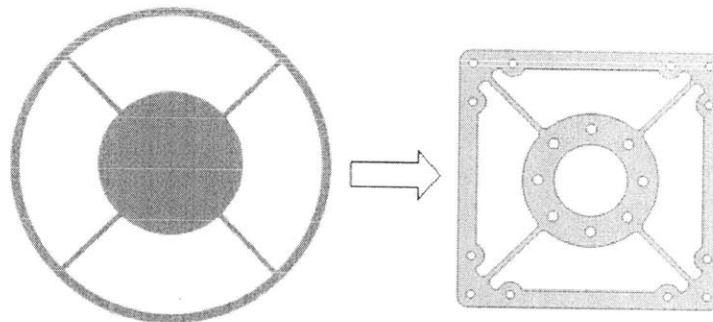
Figure 3.4: Cartwheel flexure transition

3.4 β-Prototype

3.4.1 Initial Design

In order to minimize the overall machine cost and build time, most of the components were designed to be Waterjet cut out of 12.7 mm polycarbonate. For larger pieces which would have to resist higher moment loads, rectangular aluminum tubes were used for their high stiffness, low cost, and low weight.

There are 4 subassemblies, or stages, to the beta-prototype device, shown in figure 3.5. The first stage is the base, which is a 12.7 mm thick aluminum plate. The second stage is mounted to the base and allows for rotation about the y-axis. The third stage mounts onto the second stage and rotates about the z-axis. The last stage, which holds the foot plate, mounts onto the third stage and rotates about the x-axis. Stages 2-4 all consist of a 25.4 mm x 50.8 mm x 3.175 mm (wall thickness) tube with waterjetted polycarbonate components bolted on.
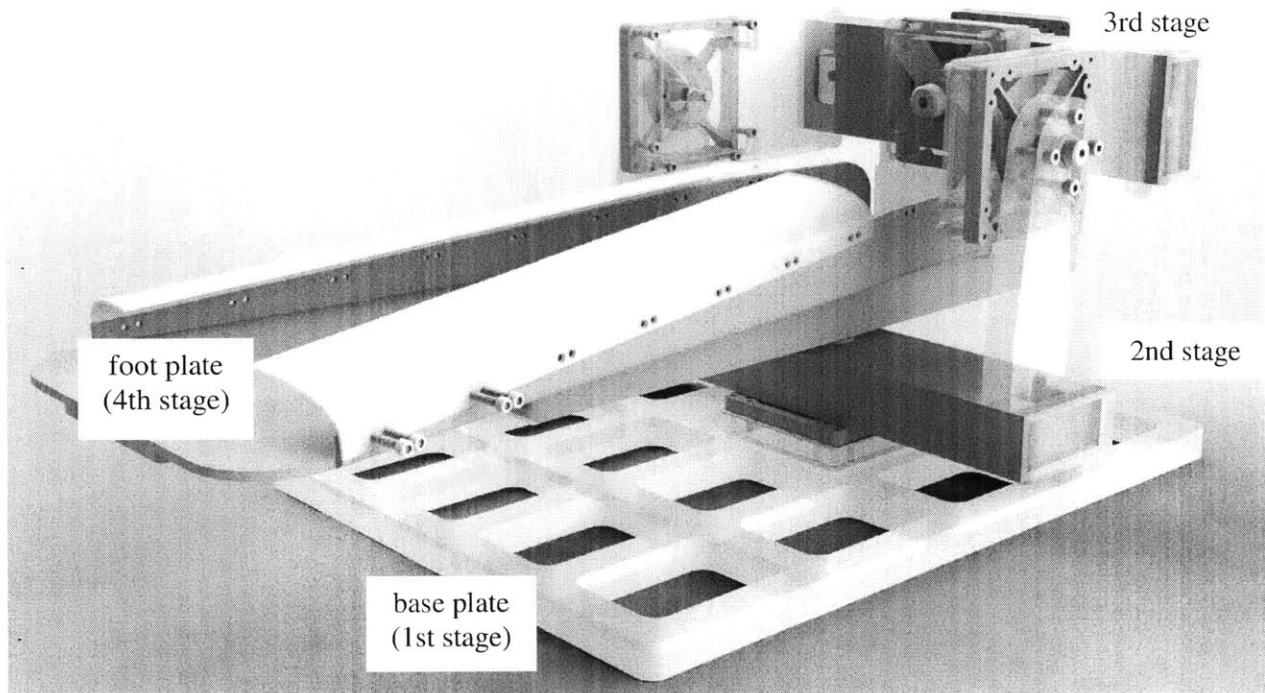
Figure 3.5: Initial design with stages labeled

3.4.2 Finite Element Analysis (FEA) and Shortcomings

First-order FEA was done on the polycarbonate pieces. Parts were isolated and static load cases with the patient's weight were simulated. For a typical polycarbonate part, this resulted in a maximum deflection of 0.2 mm, which is not significant when the end of the foot plate is expected to deflect more than 12.7 mm.

However, the β-prototype failed to be rigid enough as well. After further investigation it became apparent that torsional loading cases had not been appropriately modeled. While deflections on the order of 0.2 mm in the components are negligible, 0.2 mm at a radial arm of 25.4 mm allows an unwanted deflection of about 2.4 mm at the end of the foot plate (radial arm of 305 mm).

Additionally, the interface between the first (base) and second stages also had backlash that propagated throughout the structure. There were two sources of backlash, one of which is

that the second stage was constrained by one shoulder bolt in a single shear configuration. The second source of backlash was that the pin joint had too much clearance. The inner diameter of the bushings was about 0.127 mm larger than the diameter of the shoulder bolt, which allowed about 0.005 rad of unwanted rotation.

3.4.3 Angle Adjustment Mechanism

Shortly after the β-prototype was built, the customer requested that the device be made capable of testing ankle performance from different initial positions (plantarflexion or dorsiflexion) of the joint. Because the polycarbonate parts had to be remade with a more rigid material, it was decided to add in a basic spring-loaded pin-and-dial angle adjustment mechanism, such as is commonly seen in weight lifting machines, for the plantar/dorsiflexion mode. A close-up of the adjustment mechanism is shown in Figure 3.6.
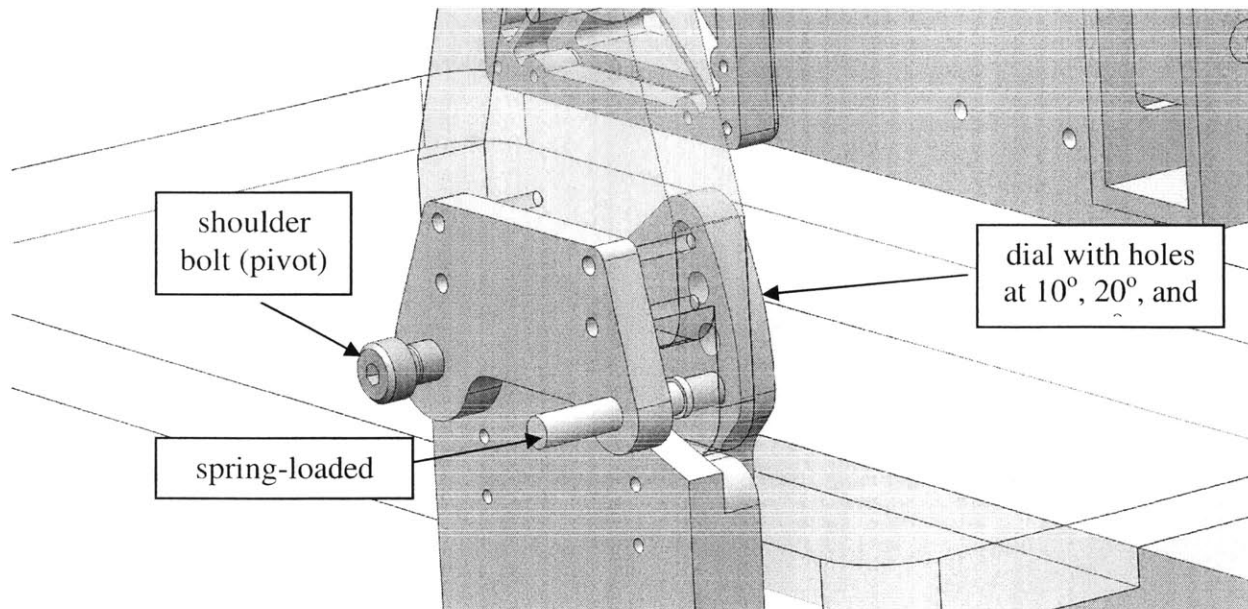
Figure 3.6: Close-up of pin-and-dial mechanism

Other modifications included elimination of spacers and changing the shoulder bolt mount such that it was now in a double shear configuration. A rendering of the resultant device is shown in Figure 3.7.
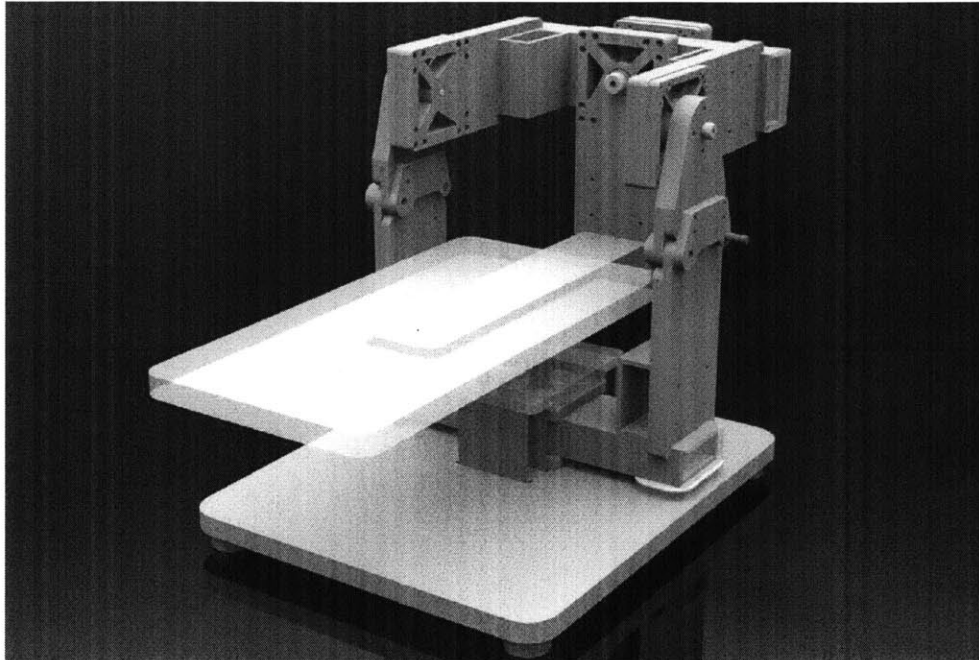
Figure 3.7: Rendering of β-prototype

Although the addition of the angle adjustment mechanism provided a better understanding of the device's potential, it also significantly increased the amount of backlash present in the machine. In order for the pins to easily slide in and out of the dial, the holes had to be made oversize by about 0.76 mm.

3.4.4 Modifications to Prototype

In order to run preliminary trials, it was crucial that backlash be mitigated further in order to minimize errors and improve the reliability and accuracy of data gathered from test subjects.

Backlash would also have added instability to the platform, which would have interfered with trials and the comfort-level of patients. Therefore two major changes were made to the prototype:

1. Removal of the y-axis rotation.

2. Installation of a leadscrew based angle adjustment mechanism.

The y-axis rotation was removable because it is not a critical component of ankle kinematics. For the proof-of-concept trial, it was sufficient to demonstrate the capability of the device to measure ankle output for plantar/dorsiflexion and inver/eversion. However, in the final version of the device, the y-axis rotation will be added back in for full diagnostics functionality. Figure 3.8 shows a close-up of the lead-screw angle adjustment mechanism.
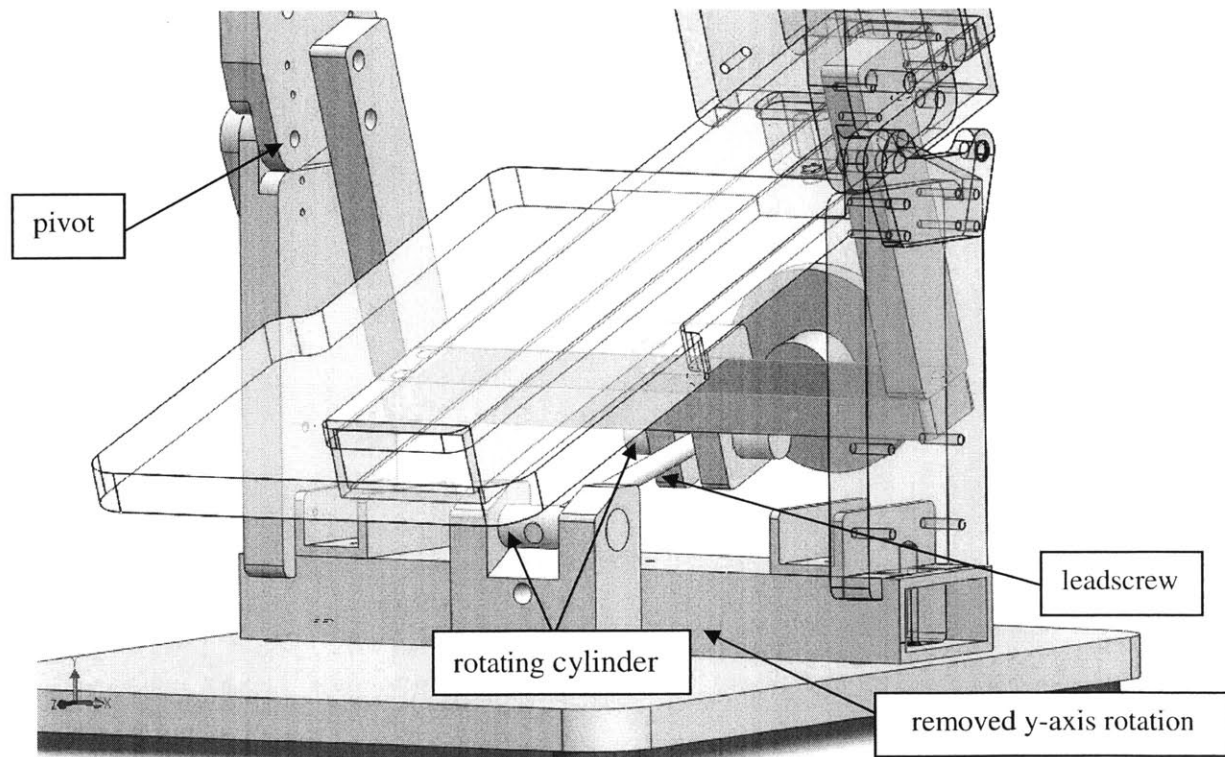
Figure 3.8: close-up of lead-screw angle adjustment mechanism

3.5 Cartwheel Flexure Evolution

During preliminary testing, a subject applied a large impulse load to the device by simulating the first half of a jumping motion. Because the cartwheel flexure had only been rated for 11.3 N-m of torque, the flexure blades snapped. The original cartwheel flexures were adequate for the x-axis (inver/eversion) and y-axis rotational modes, but not for the z-axis (plantar/dorsiflexion) rotation because it consisted of much greater force applied over a greater rotation.

In order to improve the performance of the flexures, their load capacity and range-of-motion needed to be increased. We used 45 kgf (half the maximum weight of a subject), and a moment arm of 178 mm as the upper bounds for the load (horizontal distance from true ankle joint to front sole). Therefore we can expect to see a maximum of 79 N-m of applied torque. Since the device uses two flexures per rotation, each flexure must be able to support 39.5 N-m.

3.5.1 Material Selection

The performance of the cartwheel flexures depends on two properties – the Young's Modulus E, and the yield stress σ_y. A lower young's modulus allows the flexure blade to deflect further under a given load; and a higher yield strength allows the flexure blade to have increased load capacity. Therefore materials with a low ratio of $\frac{E}{\sigma_y}$ will perform the best. Other factors to consider are fatigue, cost, material availability, and machinability. Material properties are shown in Table 3.3.

Table 3.3: Material comparison chart

material	E (MPa)	σ_y (MPa)	E/ σ_y	Fatigue	$/6.35mm x 76.2mm x 1.8m	machinability
6061-T6 Al	69000	276	250	Low	45.62	95 Brinell
7075-T6 Al	69000	455	158	Med	162.05	150 Brinell
5160 Spring Steel	205000	669	306	High	36.64	Rockwell C30
4140 Steel	205000	414	495	Med	68.29	Brinell 243
Titanium grade 5	117000	827	142	Med	853.13	Rockwell C32

Although titanium has the best ratio of $\frac{E}{\sigma_y}$, its material cost is extremely high.

Additionally, titanium and steel are very tough to machine, which drives up the waterjetting cost. While, later, the finalized product may use higher performance materials, 7075-T6 Al is the best material all around for prototyping.

3.5.2 Fatigue Performance

The fatigue life of 705-T6 Al was calculated and graphed in Figure 3.10. Because we expected to replace the cartwheel flexures after each trial, we decided to design for a safety factor of 1.5, which corresponds to approximately 1000 cycles.
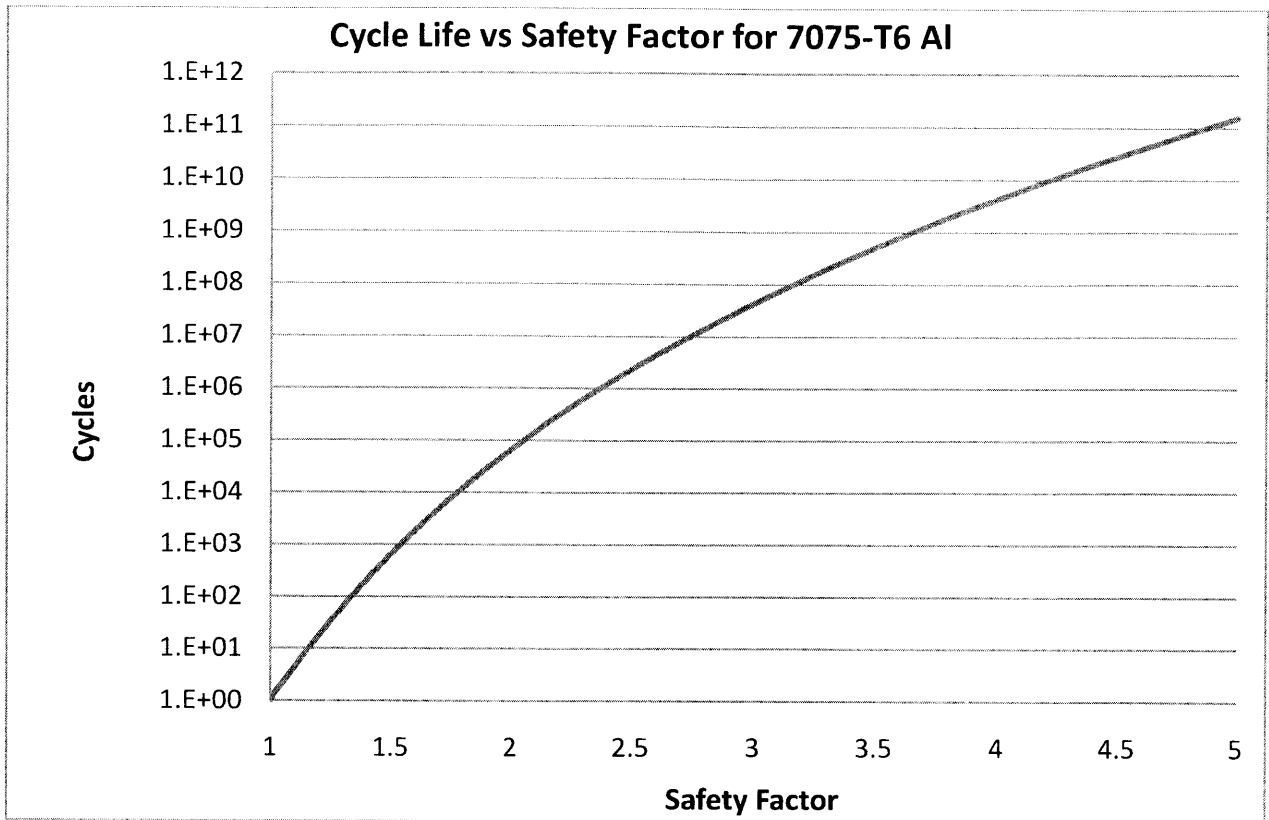
Figure 3.9: Cycle life versus safety factor for 7075-T6 Al

3.5.3 Flexure Geometry

In order to increase the rotation, a variety of cartwheel flexures with nested blades were designed and optimized with FEA. The more blades that are placed in series, the larger the range-of-motion will be for a given load capacity. Additionally, because the basic straight radial blade geometry is preserved, the angular displacement will still be linear with the applied torque. However, there are also space and fabrication considerations which must be accounted for.

Two designs were chosen for the plantar/dorsiflexion and inver/eversion axes. The results of the finite element analysis are shown in Figure 3.11, with the relevant parameters shown in Table 3.4.
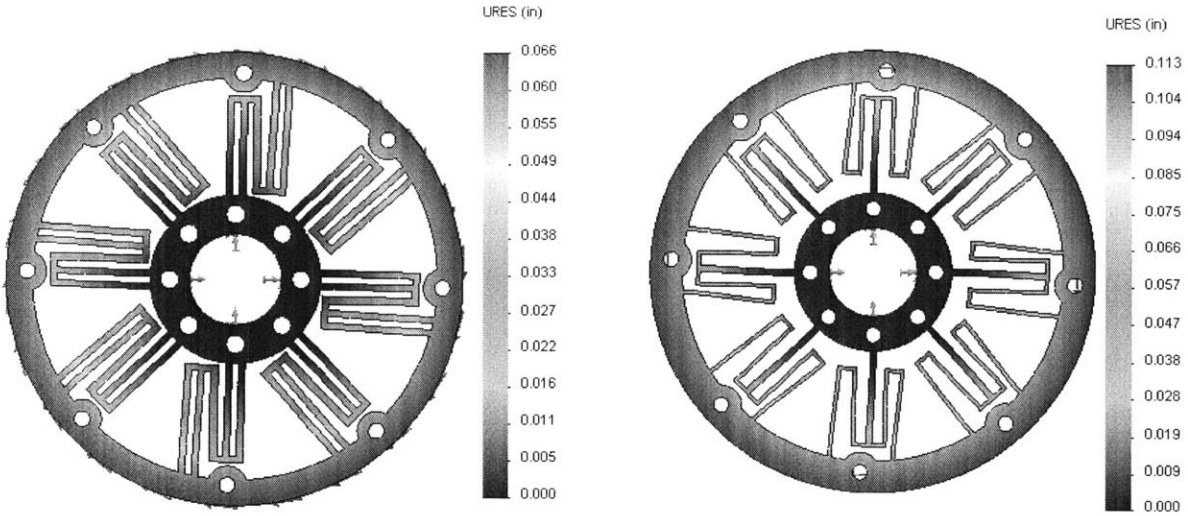
Figure 3.10: FEA of plantarflexion flexure (left) and inversion flexure (right)

Although the maximum expected torque is 39.5 N-m per cartwheel flexure, it was not expected that there would be a test subject in our preliminary trials that would be able to exert the maximum torque. Therefore, to maximize range-of-motion the cartwheel flexure for plantar/dorsiflexion was designed for an average person's maximum output torque of 28.3 N-m, using 45 kgf as half the weight and 128 mm as the moment arm. This torque is calculated for when a person is standing on the front soles of his feet.

Table 3.4: Flexure FEA results

Parameter	Plantarflexion Flexure	Inversion Flexure
Load	28.3 N-m	11.3 N-m
SF	1.5	1.5
ΔAngle	0.038 rad	0.065 rad

3.5.4 Flexure Geometry

To confirm the results of the FEA, a simple beam bending calculation was done. A simplified deformation model of a flexure blade is seen in Figure 3.12. Deflection of the flexure

31

blade is given by Equation 1, which is a modified version of the standard cantilevered beam bending equation.

$$\delta = \frac{2F\left(\frac{L}{2}\right)^3}{3EI} = \frac{FL^3}{12EI}$$

(3.1)

Figure 3.11: Deformed flexure blade

For the plantarflexion flexure, there are five blades in total: one middle blade and two blades in parallel attached to both the inner and outer hubs. Therefore $F_{applied} = F/2$. F is taken to be the force at the middle of the blades, which is at a distance 25.4 mm radially: 28.3 N-m / 25.4 mm = 1114 N. The modified displacement equation becomes:

$$\delta = \frac{2F(\frac{L_{middle}}{2})^3}{3EI_{middle}} + 2\frac{2\frac{F}{2}(\frac{L_{outer}}{2})^3}{3EI_{outer}} = \frac{F}{12E}(\frac{L_{middle}^3}{I_{middle}} + \frac{L_{outer}^3}{I_{outer}})$$

(3.1)

$$\delta = \frac{1114N}{12 * 69000 * 10^6 MPa}\left(\frac{(8.89mm)^3}{1.87mm^4} + \frac{(10.2mm)^3}{1.08mm^4}\right) = 1.73mm$$

(3.1)

As the radius of the flexure is 1.75", the cartwheel flexure is predicted to rotate 0.038 rad under the maximum load of 28.3 N-m, which is the same as the FEA result.

For the inversion flexure, the blades are in a "w" shape, with the outer and inner blades in parallel. Thus $F_{applied\ to\ outer\ and\ inner\ blades} = F/2$ again. The modified equation becomes:

32

$$\delta = \frac{2F(\frac{L_{middle}}{2})^3}{3EI_{middle}} + \frac{2\frac{F}{2}(\frac{L_{outer}}{2})^3}{3EI_{outer}} + \frac{2\frac{F}{2}(\frac{L_{inner}}{2})^3}{3EI_{inner=outer}}$$

$$= \frac{F}{12E}(\frac{L_{middle}^3}{I_{middle}} + \frac{L_{outer}^3 + L_{inner}^3}{2I_{outer}})$$

(3.1)

$$\delta = \frac{445N}{12 * 69000 * 10^6 MPa}\left(\frac{(9.40mm)^3}{1.08mm^4}\right.$$

$$\left. + \frac{(12.7mm)^3 + (7.62in)^3}{2 * 0.234mm^4}\right) = 3.05 \, mm$$

(3.1)

This corresponds to 0.068 rad of rotation, which is quite close to the FEA result.

4

RESULTS

4.1 Measurements and Data

First, the flexures were calibrated using the setup described in section 2.2. The resultant

data is shown in figures 4.1 and 4.2.

Calibration for Plantar/Dorsiflexion Flexure

$y = 0.0564x + 0.2018$

Output Voltage (V)

Applied Torque (N-m)
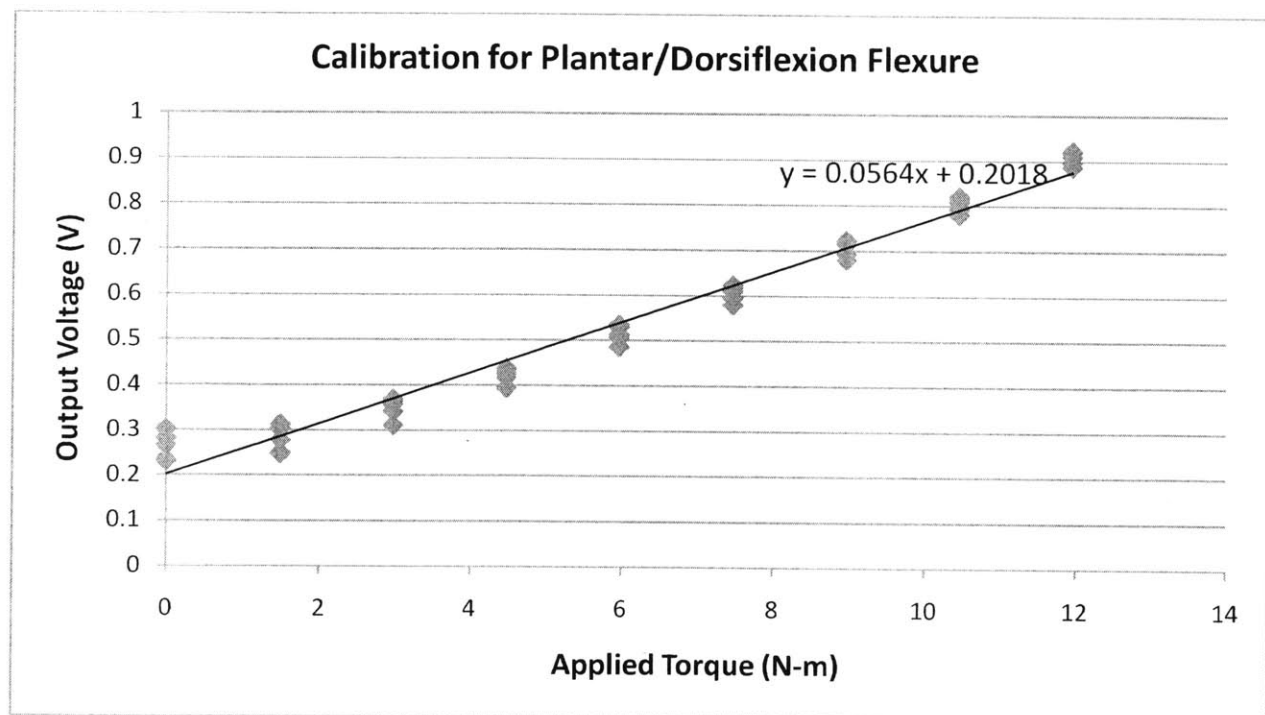
Figure 4.1: Plantar/dorsiflexion flexure calbiration data and fit line

Figure 4.2: Inver/eversion flexure calibration data and fit line

During experimentation, four test subjects were asked to stand on the device with feet placed approximately shoulder width apart. One foot was strapped into the device while the other foot rested on a platform of equal height. The subjects were then asked to exert force in the plantarflexion direction and to hold for about 20 seconds. Then the process was repeated for the dorsiflexion, inversion, and eversion directions. Data for subject 1 is shown in figure 4.3. Because the modes of ankle movement are coupled, application of torque about one axis also results in some torque being applied in the other axis as well. The maximum torques for each mode of movement and their coupled torques for the four subjects were organized into tables 4.1-4.4. All data is in N-m.
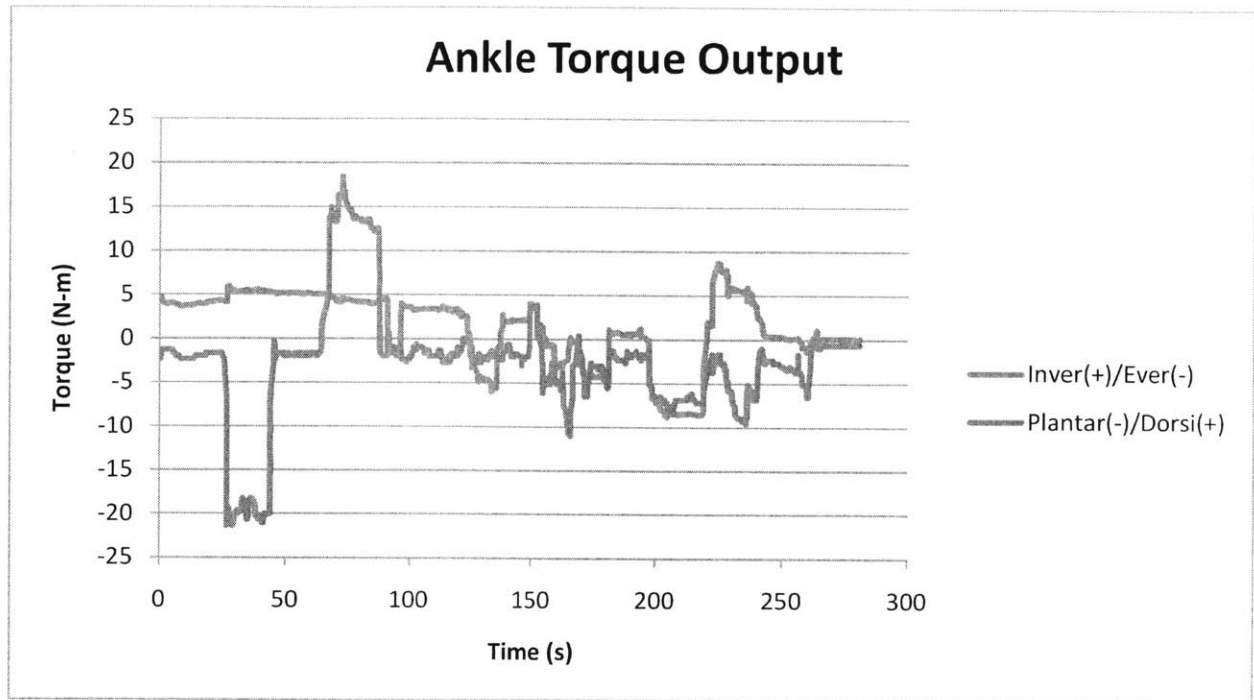
Figure 4.3: Ankle joint torque output for subject 1

Table 4.1: Subject 1 - female 47.6 kg - maximum torque values

Mode	Plantar.	Dorsi.	Inver.	Ever.
Max Plantar.	20	0	5	0
Max Dorsi.	0	14	4.5	0
Max Inver.	5	0	6	0
Max Ever.	7	0	0	8

Table 4.2: Subject 2 - male 70.3 kg - maximum torque values

Mode	Plantar.	Dorsi.	Inver.	Ever.
Max Plantar.	42	0	4	0
Max Dorsi.	0	19	0	2.5
Max Inver.	7.5	0	12	0
Max Ever.	4.5	0	0	9

Table 4.3: Subject 3 - male 72.6 kg - maximum torque values

Mode	Plantar.	Dorsi.	Inver.	Ever.
Max Plantar.	37	0	3.5	0
Max Dorsi.	0	28	0	3
Max Inver.	25	0	12	0
Max Ever.	23	0	0	12.5

Table 4.4: Subject 4 - male 81.6 kg - maximum torque values

Mode	Plantar.	Dorsi.	Inver.	Ever.
Max Plantar.	47	0	3	0
Max Dorsi.	0	37	7.5	0
Max Inver.	6	0	12	0
Max Ever.	5	0	0	10

4.2 Error Modeling

Exert the same downward force multiple times on a single point on the foot plate, and the device will measure the exact same torque each time. However, it is unlikely that users will be able place their feet in the device exactly the same each time they use it. Because alignment of foot with the device is done visually, the rotational axes of the ankle joint will always be slightly misaligned with those of the device.

All of the test data was taken with the subjects' feet in a horizontal starting position. For small angular displacements, ankle torque can be thought of as a downward force applied at the front sole of the foot. Therefore vertical alignment of the rotational axes can be neglected in the analysis for this trial.

The horizontal alignment, on the other hand, can be off by as much as 5 mm in both the x and z axes. The error from rotational axis misalignment is a percentage function of the subject's foot's moment arm (horizontal distance from rotational axis to front sole of foot). For example, for the average moment arm of 128 mm, if the subject's foot is misaligned in the positive x direction by 5 mm, the torque applied in the plantarflexion direction will be greater by $\frac{5}{128+5} =$ 3.7%. Conversely, the torque applied in the inversion direction will be smaller by 3.7%.

It should also be noted that inver/eversion errors will be greater than plantar/dorsiflexion errors because the moment arm for inver/eversion is much smaller.

Table 4.5 lists the moment arms of the test subjects and the corresponding error percentages.

37

Table 4.5: Error Percentages for Test Subjects

Subject No.	Plantar/dorsiflexion Moment Arm (mm)	Inver/eversion Moment Arm (mm)	Plantar/dorsiflexion Max Error (%)	Inver/eversion Max error (%)
1	103	35	4.8	14
2	127	51	3.9	9.8
3	130	45	3.8	11
4	135	48	3.7	10

4.3 Discussion

Inversion torques were limited to 12 N-m, at which point the foot plate collided with the side of the structure. Therefore it is expected that the maximum torque values for inversion should be higher for subjects 2-4.

The effects of joint coupling are easily observed. For all subjects, inversion and eversion motions also resulted in application of torque in the plantarflexion direction. When subjects plantarflexed, some inversion was also observed; when subjects inverted, significant plantarflexion was also observed. This suggests that the test subjects' ankle joints developed to naturally turn inwards while plantarflexing and vice-versa. It is also possible that geometric concerns such as the distance between the feet might have altered this pattern as well.

Differences in individual ankle joint development can be seen as well from these data. Eversion by subject 1 is stronger than inversion. Conversely, inversion is stronger than eversion in the other subjects. In subject 3, inversion and eversion motions resulted in the subject also applying roughly double the torque in plantarflexion. The large coupled torque suggests that subject 3's ankle joint is less developed in the directions of inversion and eversion. Therefore the ankle compensates and recruits muscles in largely the same motor pattern as seen in plantarflexion.

Subjects 2 and 3 show dorsiflexion coupling with eversion, while subjects 1 and 4 show dorsiflexion coupling with inversion. Plantarflexion did not show as much variation among the subjects. Therefore it may be the case that dorsiflexion is much more subject to individual ankle development than is plantarflexion.

5

CONCLUSIONS AND FUTURE WORK

5.1 Discussion

The purpose of the research done is to provide physicians with a diagnostics tool that can quantitatively measure the severity of an injury by measuring the ankle joint's functional output. Torque and power output have been shown to be correlated with functional performance of the ankle joint. It has been shown that the ankle rehabilitation device can measure torque output. Such a device has the potential to enable more accurate diagnoses and improve the efficacy of treatment and rehabilitation.

The device was also able to highlight the coupled motions of the AJC. Plantarflexion and inversion motions always occur jointly and are not easily isolated. Individual developments in joint development were also evident. One subject's ankle was stronger in the eversion direction than in the inversion direction, while all other subjects exhibited the reverse case. Additionally, two subjects displayed coupling between dorsiflexion and eversion while the other two subjects displayed coupling between dorsiflexion and inversion. Torque data from the device provides insight into how each subject's ankle has developed and moves, and may be very useful in a clinical setting. Further testing is needed to verify these conclusions.

Preparations for a clinical trial of the device involving a large number of patients (~50) are currently underway. This study will be used as a clinical validation of the device in addition to developing or testing relevant testing protocols beyond the scope of simply measuring

maximum torques. Subsequent analysis will be done across groups of varying age, injury status, and physical ability. Among the protocols to be evaluated are the Starr-Excursion Balance test (SEBT) and the Unipedal Stance test (UST). Range of motion cannot be measured easily with the current prototype, so this study will focus on validation. Improvements will be made so that in the γ-prototype, the range of motion will be measured through either one of two methods: (1) extremely large motion flexures (>0.5 rad); (2) a semi-automated process that depends on the torque applied. For method (2), as long as the torque applied is above a certain number, a motor will rotate the foot plate slowly; when the torque applied falls below that number, the motor will stop, and the limit of the AJC's ROM will be measurable with just the flexure's ROM.

For the clinical trial, the β-prototype will be used. After validation and any further modifications, the γ-prototype design will be finalized and built.

5.2   Areas of Improvement - Issues with β-Prototype

The initial β-prototype device was not designed to have angle adjustment capabilities. Although later on a mechanism was implemented, the rotation was about an axis that was translated from the cartwheel flexure's axis. This resulted in a misalignment error from the changing moment arm. Future mechanisms must be aligned with the cartwheel flexure's axis.

Foot sizes can vary from 178 to 330 mm long. Other dimensions such as subtalar joint and true ankle joint locations are subject to individual development. Therefore the device must be able to account for different foot geometries and sizes.

Each pair of consecutive stages in the β-prototype are connected through a pair of flexures. One stage connects to the inner ring while the other stage connects to the outer ring.

This causes flexure replacement to be complicated and difficult, as a large portion of the device has to be disassembled.

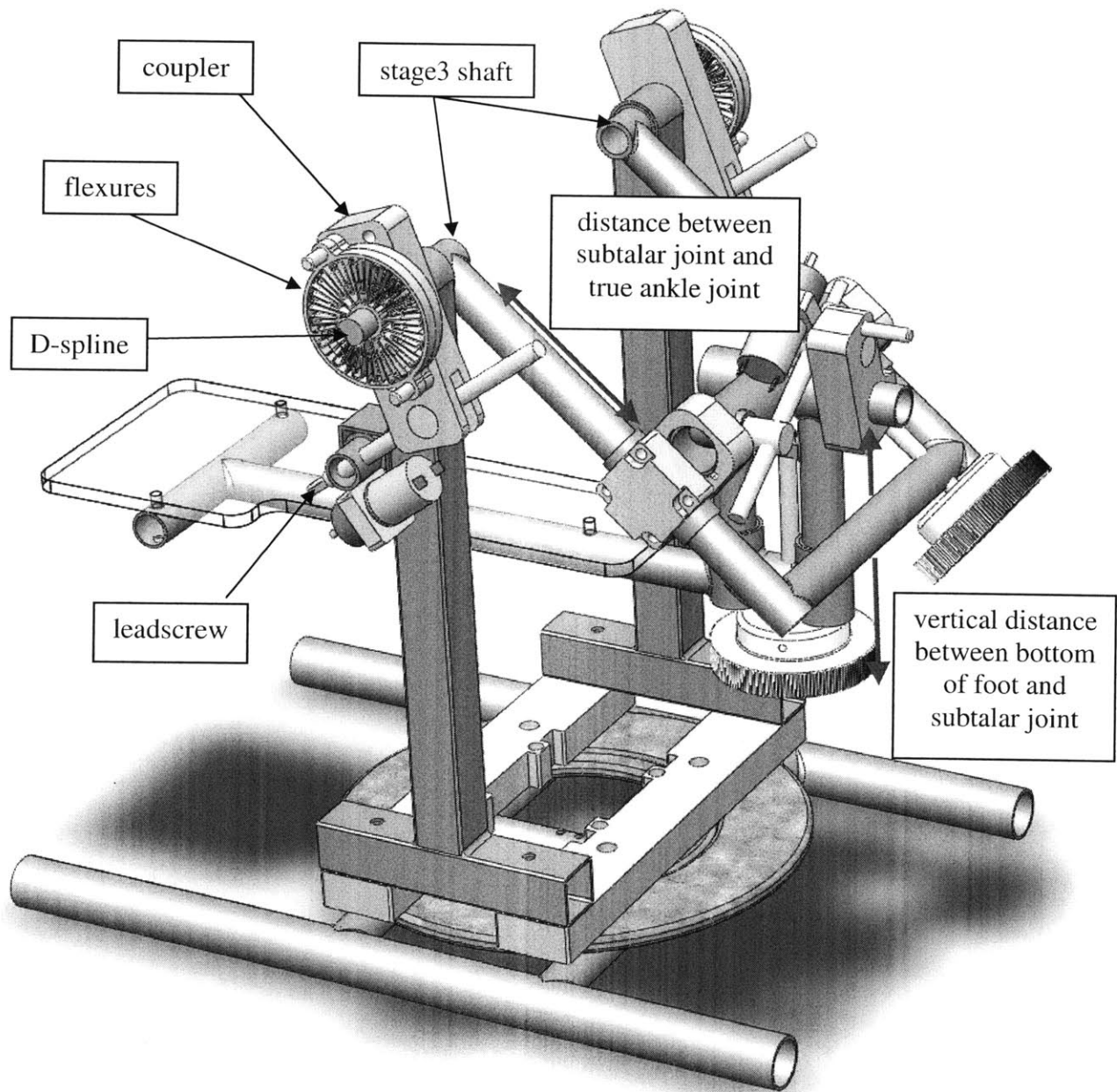To address the shortcomings of the β-prototype, a γ-Prototype was designed and is shown in Figure 5.1.

Figure 5.1: γ-prototype design

Angle adjustment is achieved with a leadscrew. The leadscrew passes through a threaded cylinder that rotates within a flexure coupler, as seen in the Figure above. The coupler is fixed to the outer ring of the cartwheel flexure by two 6.35 mm dowel pins, and is radially constrained to the shaft of stage 3. The inner ring of the flexure is fixed to stage 3 by a D-spline. When the leadscrew is turned, stage 3 and the flexure rotate together. Stage 3 also rotates within the ROM allowed by the flexure. The angle adjustment mechanism allows a ROM from -0.35 rad (dorsiflexion) to +0.79 rad (plantarflexion). A similar mechanism is added in for inver/eversion. Additionally, if the stiffness of the flexure is not high enough, i.e. it does not provide enough resistance, then additional flexures can be added on to the sides.

Stage 3 is set at 0.70 rad below the horizontal. This is because tan(0.70 rad) was chosen as an estimate for the slope from the true ankle joint axis to the rearmost point of the subtalar joint. Any deviation from this angle can be fine-tuned with the foot size adjustment mechanisms. These mechanisms control the distance between the subtalar and true ankle joints, and the distance between the subtalar joint and the bottom of the foot.

After clinical validation and trials, final adjustments will be made.

[1]   Suzuki, T., Bean, J., Fielding, R. "Muscle Power of the Ankle Flexors Predicts Functional Performance in Community-Dwelling Older Women." Journal of American Geriatric Society 49:1161-7, 2001.

[2]   Bean, J. F., Vora A., Frontera, W. R. "Benefits of Exercise for Community-Dwelling Older Adults." Archives of Physical Medicine and Rehabilitation Vol. 85 Supplement 3: 31-42, July 2004.

[3]   Griffin, L. Y. Essentials of Musculoskeletal Care. American Academy of Orthopaedic Surgeons: Sept. 2005

[4]   Holmes, A., Delahunt, E. "Treatment of Common Deficits Associated with Chronic Ankle Instability." Sports Med. 39(3): 207-24, 2009.

[5]   Ranu, H. S. "Miniature load cells for the measurement of foot-ground reaction forces and centre of foot pressure during gait." J Biomed Eng Apr; 8(2): 175-7, 1986

[6]   Girone, M., Burdea, G., Bouzit, M., Popescu, V. A. "Stewart Platform-Based System for Ankle Rehabilitation." Autonomous Robots 10: 203-12, 2001.

[7]   Deutsch, J., Latonio, J., Burdea, G., Boian, R. "Rehabilitation of Musculoskeletal Injuries Using the Rutgers Ankle Haptic Interface: Three Case Reports," Eurohaptics Conference, Birmingham UK, 6 pp. July 1-4, 2001 (in press).

[8]   Click, F. P., Bellew, J. W., Pitts, T., Kay, R. "A Comparison of 3 Hand-held Dynamometers Used to Measure Hip Abduction Strength." J Strength Cond Res 17(3): 531-5, Aug 2003.

[9]   Arndt, A., Westblad, P., Winson, I., Hashimoto, T., Lundberg, A. "Ankle and Subtalar Kinematics Measured with Intracortical Pins During the Stance Phase of Walking." Foot and Ankle International 357-365, 2004.

[10]   Ma, R., Slocum, Jr., A. H., Sung, E., Bean, J. F., Culpepper, M. L., "Torque measurement via Compliant Mechanisms". Manuscript submitted to the ASME Journal of Mechanisms and Robotics, August, 2010.

[11]   Templer, J. "The Staircase: Studies of Hazards, Falls, and Safer Design." Massachusetts, USA: MIT Press, 1992.

[12]   Ma, R., Slocum, Jr., A. H., Sung, E., Culpepper, M. L., Bean, J. F., "Ankle-Rehabilitation via Compliant Mechanisms." Conference paper and poster presentation at the Design of Medical Devices Conference in Minneapolis, MN, April 13-15 2010.

A

ELECTRONICS

A.1 Strain Gages

Catalogue page from:
http://www.omega.com/ppt/pptsc.asp?ref=SGD_LINEAR1-AXIS&Nav=pree02

To Order (Specify Model Number)

	MODEL NO.	PRICE PER PKG OF 10	NOM. RESIS-TANCE (Ω)	DIMENSIONS mm (in)† GRID A	B	CARRIER C	D	MAX V* (Vrms)	TERMINATION	TEMP COMP	TERM PAD
Shown actual size 7.80 mm	SGD-3/120-LY11	$55	120	3.00 (0.118)	1.50 (0.059)	7.80 (0.307)	3.80 (0.150)	4	Ribbon Leads	ST	BTP-3
	SGD-3/120-LY13	55	120					5.5	Ribbon Leads	AL	
	SGD-3/120-LY41	49	120	Linear pattern, grid width narrow 120 Ω				4	Solder Pads	ST	
Leads not shown	SGD-3/120-LY43	49	120					5.5	Solder Pads	AL	
Shown actual size 9.80 mm	SGD-5/350-LY11	$65	350	4.50 (0.177)	3.20 (0.126)	9.80 (0.386)	5.20 (0.205)	12	Ribbon Leads	ST	BTP-4
	SGD-5/350-LY13	65	350					17	Ribbon Leads	AL	
	SGD-5/350-LY41	55	350	Linear pattern, medium size 350 Ω				12	Solder Pads	ST	
Leads not shown	SGD-5/350-LY43	55	350					17	Solder Pads	AL	

DISCOUNT SCHEDULE

1 to 10 pkgs . . . . .Net
11 to 24 pkgs 5%
25 to 49 pkgs 10%
50 and up and OEM . .Consult Factory

* Maximum permitted bridge energizing voltage (Vrms).
Note: For strain gage accessories see pages E-56 to E-59.
Ordering Example: SGD-4/120-LY13, 3.8 mm grid, 120 Ω nominal-resistance strain gage, **$59.**

Custom-Designed Strain Gages Available! No Minimum Quantities, Consult Engineering.

NOTE
ST = Steel
AL = Aluminum

TYPICAL STRAIN GAGE INSTALLATION

Ribbon Leads from Strain Gage or User Supplied Fine Gage Wire (30 AWG) See page E-69

Instrumention Wire 20 to 28 AWG See page E-69

Adhesive, See page E-67

Bondable Terminal Pads (BTP) for Stress Relief and Junction for Different-Gage Wires, See page E-63

† Dimensions Key:

GRID
A: Active gage length
B: Active gage width
CARRIER
C: Matrix length
D: Matrix width
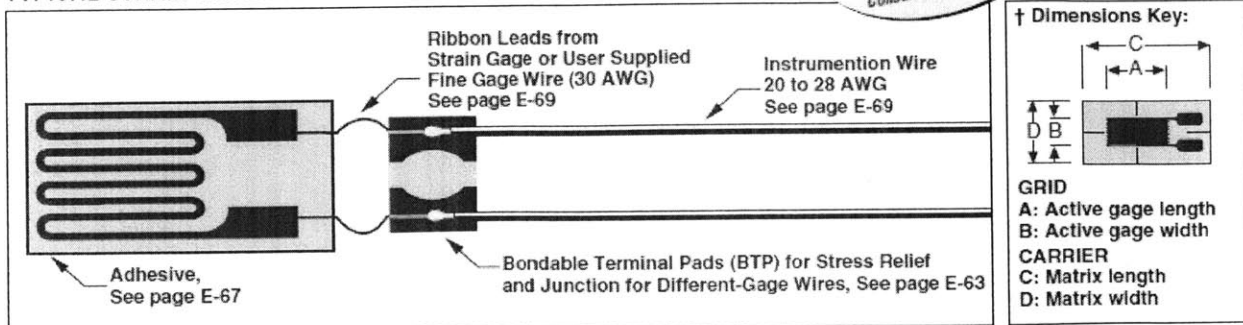
A.2 Data Acquisition Instrument

Catalogue page from:
http://www.dataq.com/products/obsolete/di194.html

DI-194RS and DI-154RS* Starter Kits — DATAQ INSTRUMENTS

Low Cost, Compact Data Acquisition Kit

### Convenient Serial Port Interface

Four ± 10V Analog Inputs

Two Digital Inputs for Remote Start/Stop and Remote Event Marker Control

The DI-194RS and DI-154RS*, DATAQ's four-channel data acquisition starter kits, are a low-cost way to experience WINDAQ software, now with more features and capabilities than ever before. With these starter kits, you can digitize virtually any transducer's analog output signal and record it to your PC's hard disk. At the same time, view the transducers output on your PCs monitor in a triggered sweep (oscilloscope-like) or scrolling (chart recorder-like) display format.

Our starter kits provide a taste of the exceptional power and speed possible with WINDAQ software. They provide 12-bit (DI-154RS) and 10-bit (DI-194RS) measurement accuracy, a ±10V analog measurement range, up to 240 samples/second throughput, and four analog input channels. A CD demonstrates WINDAQ Waveform Browser (WWB), our playback and analysis software, but to get a hands-on illustration of the data recording and display capabilities of WINDAQ/Lite, you need a DI-154RS or DI-194RS starter kit. When connected to your PC's serial port, these starter kits allow you to record, display, and analyze data using your own signals. The kits ship with WINDAQ/Lite (Recording Software and Playback and Analysis software). Data acquisition rates up to 240 samples per second are supported for Windows 2000 and XP.
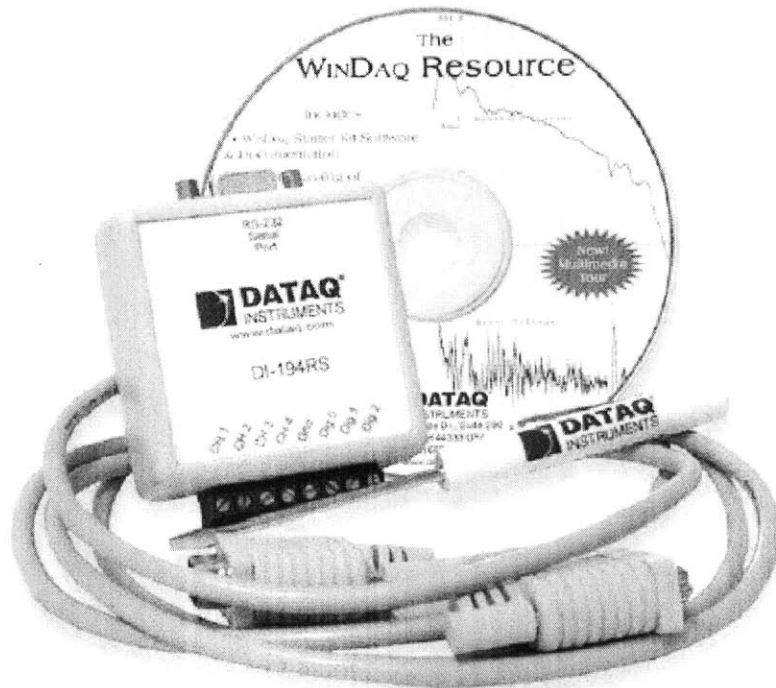
The DI-194RS Module with the WINDAQ Resource CD, screwdriver, and cable—all included with each starter kit. DI-154RS* module case is identical.

Features

Self-Powered Advantage
The DI-154RS and DI-194RS derive their power directly from the RS-232 serial port to which it is connected — no batteries to replace or external power supplies to connect.

More Capabilities
The DI-154RS and DI-194RS starter kits are equipped with two digital inputs for remote start/stop and remote event marker control.

Included ActiveX Control Library
Both starter kits are provided with an ActiveX Control Library that allows you to program the starter kits from any Windows programming environment.

Free Data Acquisition Software
Our WINDAQ/Lite data acquisition software offers real time display and disk streaming for the Windows environment. Their real time display can operate in a smooth scroll or triggered sweep mode of operation, and can be scaled into any unit of measure. Event markers with comments allow you to annotate your data acquisition session with descriptive information as you're recording to disk.

Raise your productivity to new heights with WINDAQ's unique multitasking feature. Record waveform data to disk in the background while running any combination of programs in the foreground — even WINDAQ Waveform Browser playback software to review and analyze the waveform data as it's being stored!

Specifications

WinDaq Software Specifications

Disk and Display

Max rate to disk:	Max Hardware Sample Rate
Max rate to display:	Max Hardware Sample Rate
Max data file size:	Unlimited
Display Modes:	Scrolling, freeze, triggered, non triggered. Dot-joined at all sample rates.
Storage Modes:	Continuous, pre- or post-trigger.
Display compression ratios:	1:1 to 1:9000
Displayed channels:	1 to 32
Time and Data Stamping:	Automatic
Max event markers:	8,184 per file

Waveform Display Scaling

Screen Scaling per channel:	Waveform expansion, contraction, and offset.
Engineering Units Conversion:	y=mx+b per channel

Hard Copy — print screen; continuous form

Data Storage Format — 2's complement

Waveform Measurements

Cursor-based, single-point:	Amplitude measurements per channel in calibrated units; elapsed time; time and date at cursor.
Cursor-based, dual-point:	Time measurements on the same or across different channels; D%; Y-value difference; two-point slope (d/dt); number of samples; Hz; cycles per minute.
Cursor-based (freq vs. amplitude):	Frequency vs. db; Frequency vs. magnitude (in engineering units).

Waveform Analysis

Statistics:	min; max; variance; standard deviation; mean; median; sum; sum of squares; skewness; RMS; area; slope
Frequency:	32 to 16,384 points (FFT); 2 to 8,191 points (DFT).
Advanced CODAS analysis:	Waveform integration; differentiation; arithmetic operations; rectification; moving average; peak and valley detection.

Waveform Export — WinDaq (CODAS) format to any spreadsheet (CSV), ASYST, ASYSTANT, DADiSP, CODAS, general purpose binary and ASCII.

Hardware Requirements — Any Intel or compatible PC running Windows 2000 or XP. No memory requirements beyond that required by the operating system.

Hardware Specifications*

Interface I/O	RS-232
Baud Rate	4800

Analog Inputs

Number of input channels:	4
Input type:	Single-ended
Analog Resolution:	DI-194RS: 10-bit DI-154RS: 12-bit
A/D conversion method:	Successive approximation
Sampling Rate:	240 samples/second
Relative Accuracy:	DI-194RS: 0.1% DI-154RS: 0.25%
Measurement Range:	±10V
Overvoltage Protection:	±20V peak
Input Impedance:	200k ohms

Digital Inputs

Number of inputs:	2**
Minimum high level:	3.5V
Maximum low level:	0.8V

Digital Outputs

Number of outputs:	1**

Power Requirements

Current:	Less than 4 mA
Source:	Derived from RS-232 port

Software Included

DI-194RS:	WinDaq/Lite (includes Recording and Playback software).
DI-154RS:	DI-154RS: WinDaq/Lite (includes Recording and Playback software).

*Specifications are for both the DI-194RS and DI-154RS unless noted otherwise.
**Not for general purpose use—Reserved for use by WinDaq Software.

Front End Schematic
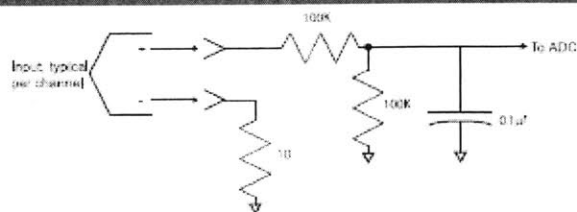
Data Acquisition Product Links

(click on text to jump to page)

Data Acquisition | Data Logger | Chart Recorder | Thermocouple | Oscilloscope

Ordering Guide

Description	Order Number
DI-194RS Starter Kit 4-channel 10-bit data acquisition starter kit.	DI-194RS
DI-154RS Starter Kit 4-channel 12-bit data acquisition starter kit.	OBSOLETE

DATAQ® INSTRUMENTS

241 Springside Drive
Akron, Ohio 44333
Phone: 330-668-1444
Fax: 330-666-5434
www.dataq.com